

# Ultra-Sparse Non-Binary LDPC Codes for Probabilistic Amplitude Shaping

Fabian Steiner\*, Gianluigi Liva†, Georg B ocherer\*

\*Institute for Communications Engineering  
Technical University of Munich

Email: {fabian.steiner, georg.boecherer}@tum.de

†Deutsches Zentrum f ur Luft- und Raumfahrt  
We bling, Germany

Email: gianluigi.liva@dlr.de

**Abstract**—This work shows how non-binary low-density parity-check codes over  $\mathbb{F}_{2^p}$  can be combined with probabilistic amplitude shaping (PAS) (B ocherer, *et al.*, 2015), which combines forward-error correction with non-uniform signaling for power-efficient communication. Ultra-sparse low-density parity-check codes over  $\mathbb{F}_{64}$  and  $\mathbb{F}_{256}$  gain 0.6 dB in power efficiency over state-of-the-art binary LDPC codes at a spectral efficiency of 1.5 bits per channel use and a blocklength of 576 bits. The simulation results are compared to finite length coding bounds and complemented by density evolution analysis.

## I. INTRODUCTION

Bandwidth-limited communication systems must use higher-order modulations such as quadrature amplitude modulation (QAM) or amplitude phase-shift keying (APSK) to provide the required spectral efficiency (SE) for high data rates. In most standards, these modulation formats are combined with uniform signaling, i.e., all points in the constellation are transmitted with the same probability. This approach loses up to 1.53 dB [1, Sec. IV] in power efficiency and lacks flexibility because it restricts the choice of SEs to supported modulation order and code rate combinations (modcods). Recently, probabilistic amplitude shaping (PAS) was proposed [2] to overcome these shortcomings: PAS closes the shaping gap and allows seamless rate adaptation by adjusting the channel input distribution. The enabling device is the distribution matcher (DM) [3] which transforms uniform input bits into arbitrarily shaped sequences. The practicality of this scheme has been demonstrated in a number of optical field trials [4]–[6] and has been proposed to 3GPP for inclusion in the upcoming 5G standard [7]. In all these works, either *binary* low-density parity-check (LDPC), turbo or polar codes [8] have been employed.

One important scenario in the upcoming standards is *ultra reliable low-latency communication* (uRLLC) [9], which requires forward error correction (FEC) with small blocklengths and very low bit error rates to guarantee the required reliability. Non-binary codes are particularly good codes in this regime of operation [10]–[12].

The combination of PAS and non-binary codes was suggested in [13]. Herein, the authors propose a new design for circular QAM constellations that can be used with non-binary codes over prime fields of order larger than two.

In this work, we propose a different strategy and consider non-binary codes over the extension field  $\mathbb{F}_q$  with  $q = 2^p$ . We illustrate the principle by ultra-sparse non-binary low-density parity-check (NB-LDPC) [14], [15] codes, which have shown an excellent performance on the binary-input additive white Gaussian noise (biAWGN) channel for short blocklengths [16]. These codes are also known as cycle codes [17] and have constant variable and check node degrees, where the former is fixed to two. Codes over  $\mathbb{F}_{2^p}$  also allow for low complexity decoding using the Hadamard transform (HT) [18].

This paper is structured as follows. Sec. II reviews the system model and introduces achievable rate expressions. In Sec. III, we show how NB-LDPC codes can be combined with PAS. Sec. IV provides numerical simulation results and a comparison with binary LDPC codes. We conclude in Sec. V.

## II. PRELIMINARIES

### A. System Model

Consider transmission over a real-valued additive white Gaussian noise (AWGN) channel

$$Y_i = X_i + Z_i \quad (1)$$

for  $i = 1, \dots, n$  channel uses. The realizations for the channel input  $X_i$  are taken from a scaled  $M = 2^m$ -ary amplitude shift keying (ASK) constellation  $\mathcal{X} = \{\pm 1, \pm 3, \dots, \pm(M-1)\}$  such that  $\mathbb{E}[X_i^2] = 1$ . The results extend directly to QAM, where we use ASK for the in-phase and quadrature transmission. The noise  $Z_i$  is a Gaussian random variable with zero mean and variance  $\sigma^2$ . The signal-to-noise ratio (SNR) is  $1/\sigma^2$ . As the channel is memoryless, we drop the index  $i$  and denote the governing channel law as  $p_{Y|X}$ . The mutual information maximizing distribution under an average power constraint is a zero mean Gaussian input  $X$  with unit variance, and it yields the capacity expression

$$C_{\text{AWGN}}(\text{SNR}) = \frac{1}{2} \log_2(1 + \text{SNR}). \quad (2)$$

To approach  $C_{\text{AWGN}}$  with discrete signaling, either geometric shaping (GS) or probabilistic shaping (PS) can be employed to mimic a Gaussian shape. In [19], we demonstrated the superiority of PS for practical coded modulation scenarios, and

we use PAS therefore. Numerical comparisons in [2, Table I] show that Maxwell-Boltzmann (MB) distributions [20]

$$P_X(x) \propto \exp(-\nu x^2) \quad (3)$$

are nearly optimal. They are also natural choices for power efficient communication, as they are the solution to the problem of minimizing the average power of the channel inputs subject to an entropy constraint.

An achievable rate for symbol-metric decoding (SMD) is

$$R_{\text{SMD}}(\text{SNR}; P_X) = I(X; Y) \quad (4)$$

where  $I(X; Y)$  is the mutual information between the channel input  $X$  and channel output  $Y$ . To use binary codes, we label each constellation point  $x \in \mathcal{X}$  with an  $m$ -bit binary label, i.e.,  $\beta: \mathcal{X} \rightarrow \{0, 1\}^m$  and  $\beta(x) = B_1 B_2 \dots B_m = \mathbf{B}$ . A binary reflected Gray code (BRGC) [21] usually performs well. An achievable rate for bit-metric decoding (BMD) is given by [22]

$$R_{\text{BMD}}(\text{SNR}; P_X) = \left[ H(\mathbf{B}) - \sum_{i=1}^m H(B_i|Y) \right]^+ \quad (5)$$

We denote the Shannon limits for (2), (4) and (5) for a fixed SE as  $\text{SNR}_{\text{CAP}}$ ,  $\text{SNR}_{\text{SMD}}$  and  $\text{SNR}_{\text{BMD}}$ , i.e.,  $R_{\text{SMD}}(\text{SNR}_{\text{SMD}}; P_X) = R_{\text{BMD}}(\text{SNR}_{\text{BMD}}; P_X) = C_{\text{AWGN}}(\text{SNR}_{\text{CAP}})$ .

### B. Distribution Matching

A DM [3] transforms uniformly distributed bits into shaped symbols. In our setup, we employ a fixed-to-fixed length DM which maps  $k$  input bits to  $n$  output symbols from the amplitude set  $\mathcal{A}$  of the  $M$ -ASK constellation. The mapping is invertible, so the input can be recovered from the output. Both the desired distribution  $P_A$  and the output length  $n$  serve as an input parameter to the DM. The matcher rate is

$$R_{\text{dm}} = k/n \quad \left[ \frac{\text{bits}}{\text{output symbols}} \right].$$

## III. NON-BINARY LDPC CODES OVER $\mathbb{F}_q$ WITH PAS

An NB-LDPC code  $\mathcal{C}$  is defined as the nullspace of the sparse parity-check matrix  $\mathbf{H}$  of dimension  $m_c \times n_c$  where the non-zero entries  $h_{ji}$  of  $\mathbf{H}$  are taken from the finite field  $\mathbb{F}_q$ , i.e.,  $\mathcal{C} = \{\mathbf{c} \in \mathbb{F}_q^{n_c} : \mathbf{c}\mathbf{H}^T = \mathbf{0}\}$ . The parity-check matrix  $\mathbf{H}$  can be represented by a bipartite graph, called the Tanner graph [23]. Every codeword symbol  $c_i$  is represented by one of the  $n_c$  variable nodes  $V_i$  in the graph. The  $m_c$  linear constraints are represented by check nodes  $C_j$ . If the edge label  $h_{ji}$  is non-zero, then there is an edge between  $V_i$  and  $C_j$ . Variable and check node  $V_i$  and  $C_j$  have degree  $d_{v,i}$  and  $d_{c,j}$ , respectively, where the degree specifies the number of associated edges. In the following, we use a special class of NB-LDPC codes, namely ultra-sparse regular LDPC codes, which have a constant variable node degree of  $d_{v,i} = d_v = 2$  and a constant check node degree  $d_c$ . Their design rate is therefore  $1 - 2/d_c$ . Previous works have shown that this ultra-sparse structure facilitates the design of graphs with a large

girth [24], which is the length of the smallest cycle in the bipartite graph and important for iterative decoding. Although their minimum distance scales only logarithmically with the blocklength [16, Sec. IV-E], numerical simulation results show lower error floors than their binary counterparts. We assume a probability-domain based decoding.

### A. PAS with NB Codes: Rate $(m-1)/m$

The PAS system model is depicted in Fig. 1. It exploits the symmetry property of the optimal input distribution  $P_X$  to factorize the random variable  $X$  into independent random variables referring to the amplitude and sign (*amplitude-sign factorization*), i.e.,  $P_X(x) = P_A(|x|)P_S(\text{sign}(x))$ . The sign distribution  $P_S$  is uniform on  $\mathcal{S} = \{-1, +1\}$ , while  $P_A$  is non-uniform on the amplitude set  $\mathcal{A} = \{1, 3, \dots, 2^m - 1\}$ . See [2, Sec. III-IV] for further details.

We first use  $R_c = (m-1)/m$  codes with a  $2^m$ -ASK constellation. In Fig. 1, this corresponds to  $\gamma = 0$ . The DM maps  $k$  data bits to  $n$  amplitudes. The FEC encoder generates redundancy, which is mapped to the  $n$  signs. FEC encoding is systematic, to preserve the amplitude distribution imposed by the DM. The combination of an amplitude and a sign results in one channel input symbol. The  $n$  channel input symbols can be represented by  $mn$  bits, which requires an NB code with blocklength  $n_c = (nm)/p$ .

Each amplitude requires  $(m-1)$  bits for its representation and we require  $p = \ell(m-1)$  when  $2^m$ -ASK PAS is combined with NB codes over  $\mathbb{F}_q$ . The variable  $\ell \in \mathbb{N}$  defines the number of amplitudes in  $\mathcal{A}$  which are mapped to one  $\mathbb{F}_q$  symbol. We denote this mapping as

$$\beta_A: \mathcal{A}^\ell \rightarrow \mathbb{F}_q. \quad (6)$$

The amplitude part has a size of  $k_c = n/\ell$  symbols and is collected in vector  $\mathbf{u} \in \mathbb{F}_q^{k_c}$ . Systematic encoding with  $\mathbf{G} = (\mathbf{I} \ \mathbf{P})$  yields the parity part  $\mathbf{p} = \mathbf{u}\mathbf{P}$  of  $(1-c)n_c$  symbols that are approximately uniformly distributed [13, Theorem I]. We will therefore assume at the decoder that the signs are uniformly distributed. Using the inverse of the mapping

$$\beta_S: \{0, 1\}^p \rightarrow \mathbb{F}_q \quad (7)$$

we relate each parity symbol to a sign sequence.

For the decoder input we need to calculate the vectors

$$\mathbf{P}_i = \begin{pmatrix} P_{C_i|Y}(0|\mathbf{y}) \\ P_{C_i|Y}(1|\mathbf{y}) \\ \vdots \\ P_{C_i|Y}(\alpha^{q-2}|\mathbf{y}) \end{pmatrix}, \quad i = 1, \dots, n_c \quad (8)$$

where  $\alpha$  refers to a primitive element of  $\mathbb{F}_q$ , i.e.,  $\mathbb{F}_q = \{0, 1, \alpha, \dots, \alpha^{q-2}\}$ . The value  $P_{C_i|Y}(c|\mathbf{y})$  denotes the probability that the  $i$ -th codeword symbol is  $c$ , when  $\mathbf{y}$  was received.

We need to distinguish two cases for the soft-input vectors  $\mathbf{P}_i$  depending on whether the codeword symbol  $c_i \in \mathbb{F}_q$  refers to an amplitude (6) or sign mapping (7). Let  $\mathbf{y}_i^A = (y_1, \dots, y_\ell)$  be the vector of all received symbols that resulted from the transmission of the amplitudes associated with the  $i$ -th codeword symbol. Similarly, the vector  $\mathbf{y}_i^S = (y_1, \dots, y_p)$  refers

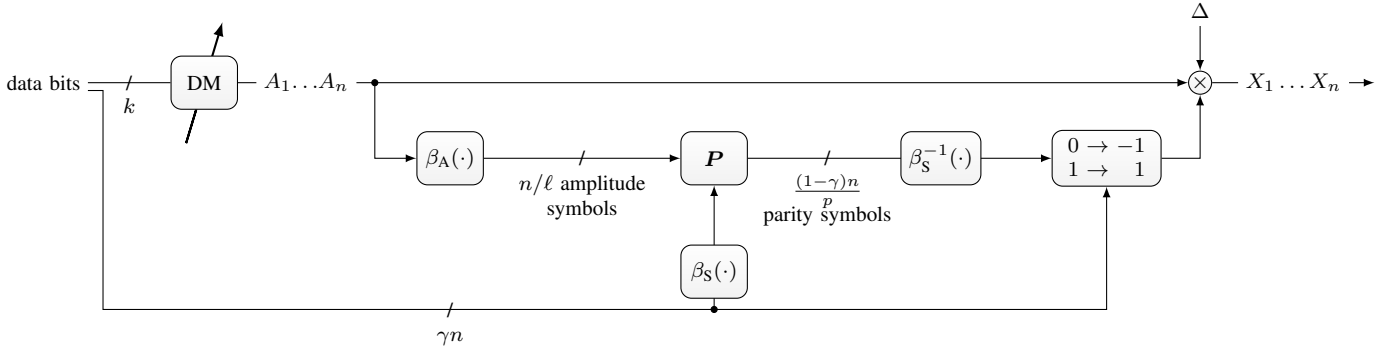


Fig. 1. System model of PAS for NB  $\mathbb{F}_q$  codes and  $q = 2^p$ .

to the received symbols that resulted from the transmission of the signs associated with the  $i$ -th codeword symbol.

a) *Amplitude Mappings*: For  $i = 1, \dots, k_c$  and  $\mathbf{a} = (a_1, \dots, a_\ell) = \beta_A^{-1}(c)$ , assuming uniform signs, the demapper calculates the metric

$$\begin{aligned}
 P_{C_i|Y}(c|\mathbf{y}_i^A) &\propto P_{C_i,Y}(c, \mathbf{y}_i^A) = P_{AY}(\beta_A^{-1}(c), \mathbf{y}_i^A) \\
 &= \prod_{j=1}^{\ell} P_{AY}(a_j, y_j) \\
 &= \prod_{j=1}^{\ell} \sum_{s \in \{\pm 1\}} P_{XY}(a_j s, y_j) \\
 &= \prod_{j=1}^{\ell} \frac{1}{2} P_A(a_j) \sum_{s \in \{\pm 1\}} p_{Y|X}(y_j | a_j s). \quad (9)
 \end{aligned}$$

b) *Sign Mappings*: For the parity part  $i = k_c + 1, \dots, n_c$  and  $\mathbf{s} = (s_1, \dots, s_p) = \beta_S^{-1}(c)$ , assuming uniform signs, the demapper calculates the metric

$$\begin{aligned}
 P_{C_i|Y}(c|\mathbf{y}_i^S) &\propto P_{C_i,Y}(c, \mathbf{y}_i^S) = P_{SY}(\beta_S^{-1}(c), \mathbf{y}_i^S) \\
 &= \prod_{j=1}^p P_{SjY}(s_j, y_j) \\
 &= \prod_{j=1}^p \sum_{\substack{x \in \mathcal{X}: \\ \text{sign}(x) = s_j}} P_{XY}(x, y_j) \\
 &= \prod_{j=1}^p \frac{1}{2} \sum_{a \in \mathcal{A}} P_{Y|X}(y_j | a s_j) P_A(a). \quad (10)
 \end{aligned}$$

We illustrate the setting for  $(m-1)/m$  codes and a  $2^m$ -ASK constellation in Fig. 2 for  $m = 3$ . We consider a code over  $\mathbb{F}_{16}$  ( $p = 4$ ) and a blocklength of three symbols. Then, each of the two symbols in the information part represents  $\ell = 4/(3-1) = 2$  amplitudes. The last codeword symbol forms the parity part and is mapped to four sign bits.

#### B. PAS with NB Codes: Rates Larger Than $(m-1)/m$

As for the binary case, PAS can also be operated with non-binary codes of rates larger than  $(m-1)/m$ . In this

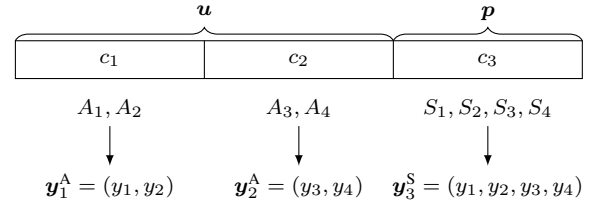


Fig. 2. Illustration how the codeword symbols of a  $\mathbb{F}_{16}$  code are associated with amplitudes and signs for 8-ASK with PAS. For the codeword length of 3 symbols, four channel inputs  $X_i = A_i S_i$ ,  $i = 1, \dots, 4$  can be generated.

case,  $(\gamma n)/p$  information symbols are used as signs, where [2, Sec. IV-D]

$$\gamma = 1 - (1-c)m. \quad (11)$$

This means (9) must only be applied for the first  $n/\ell$  variables nodes (nodes associated with amplitude mappings) and the remaining  $n/p$  variable nodes (nodes associated with sign mappings) are initialized with (10).

The overall transmission rate of a PAS transmitter is therefore

$$R_t = R_{\text{dm}} + \gamma \quad (12)$$

and the large flexibility in supported SEs is achieved by using different DM rates  $R_{\text{dm}}$  for the same FEC.

#### IV. FINITE LENGTH SIMULATIONS

We now present simulation results for ultra-sparse NB-LDPC codes over  $\mathbb{F}_{64}$  and  $\mathbb{F}_{256}$ . The considered codes are short, so we must account for the rate loss of the DM [3], which is

$$R_{\text{loss}} = H(P_A) - k/n. \quad (13)$$

To obtain a desired rate  $R_t$  and to mitigate the rate loss, we tune the parameter  $\nu$  of the MB distribution  $P_A(a) \propto \exp(-a^2 \nu)$ ,  $a \in \{1, 3, \dots, M-1\}$  to support the desired rate  $R_{\text{dm}} = R_t - \gamma$ .

#### A. Finite Length Bounds

To benchmark the finite length performance we use Shannon's sphere packing bound (SPB) [25] on the average frame

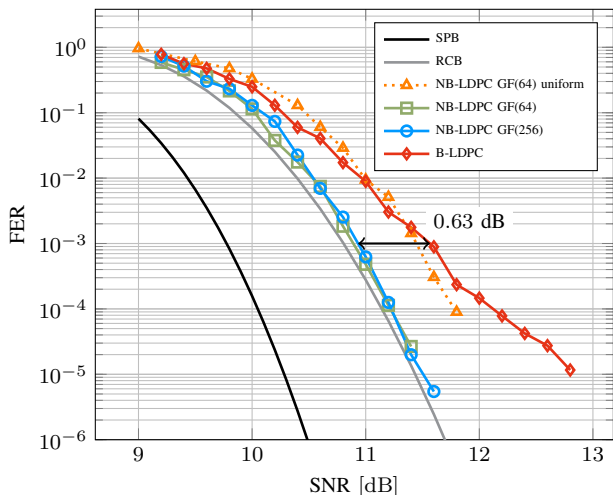


Fig. 3. Simulation results of suggested NB-LDPC coding scheme for 8-ASK,  $R_t = 1.5$  bpcu and binary blocklength of  $n_{c,\text{bin}} = 576$  bits.

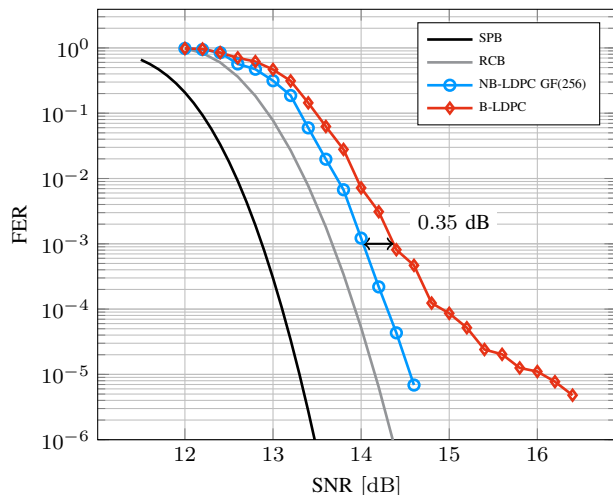


Fig. 4. Simulation results of suggested NB-LDPC coding scheme for 8-ASK,  $R_t = 2.0$  bpcu and binary blocklength of  $n_{c,\text{bin}} = 768$  bits.

error rate (FER)  $P_B$  and Gallager's random coding bound [26, Theorem 5.6.2]. The latter is

$$E[P_B] \leq 2^{-nE_G(R_t, P_X)} \quad (14)$$

where the Gallager exponent is calculated as

$$E_G(R_t, P_X) = \max_{\rho \in [0,1]} -\log_2 \left( \int_{-\infty}^{\infty} \left( \sum_{x \in \mathcal{X}} p_{Y|X}(y|x)^{\frac{1}{1+\rho}} P_X(x) \right)^{(1+\rho)} dy \right) - \rho R_t.$$

The distribution  $P_X$  is the one chosen to guarantee the desired SE  $R_t$ .

### B. Numerical Results

We compare the FER of our NB-LDPC codes with the binary LDPC codes suggested for 5G by Qualcomm [27]. The latter codes are protograph-based [28] and constructed via liftings from a set of three base matrices for low, medium and high code rates. These base matrices have two punctured (state) and degree one variable nodes. This construction yields a significant performance improvement in the waterfall region [28]. Two hundred belief propagation (BP) iterations were used. The codes were derived from the high-rate basematrix of the proposal [27] and have girth 4 ( $n_{c,\text{bin}} = 576$ ,  $R_c = 3/4$ ) and 6 ( $n_{c,\text{bin}} = 768$ ,  $R_c = 3/4$ ;  $n_{c,\text{bin}} = 1008$ ,  $R_c = 5/6$ ).

The non-binary LDPC codes were constructed from protographs of the form

$$\underbrace{[2 \quad 2 \quad \dots \quad 2]}_{d_c/2}$$

via cyclic liftings and a progressive edge-growth (PEG)-like algorithm [29]. All constructed matrices have girth 8. The coefficients were optimized row-wise by following the binary image approach of [16]. As in the binary case, we performed a maximum of 200 BP iterations for decoding. The parameters are summarized in Table I.

Fig. 3 shows simulation results for a blocklength of  $n_{c,\text{bin}} = 576$  bits and  $R_t = 1.5$  bpcu. We first compare two  $\mathbb{F}_{64}$  codes ( $n_c = 96$  symbols), where the green line with squares refers to the shaped scenario with a rate  $3/4$  ( $d_c = 8$ ) code, whereas the orange line with triangles is its uniform counterpart of rate  $1/2$  ( $d_c = 4$ ). The shaped case clearly improves over the uniform one. We also show a curve for a  $\mathbb{F}_{256}$  code of rate  $3/4$  which has almost the same performance as the  $\mathbb{F}_{64}$  version. These results are complemented by a Monte Carlo density evolution (DE) analysis which yields asymptotic decoding thresholds of 9.54 dB (uniform), 8.76 dB (shaped,  $\mathbb{F}_{64}$ ) and 8.79 dB (shaped,  $\mathbb{F}_{256}$ ). The latter two thresholds only exhibit a gap of about 0.3 dB to the respective Shannon limit (cf. Table I). Comparing both NB approaches to the binary LDPC code, we see an improvement of 0.63 dB at a FER of  $10^{-3}$ . The same DM with the same shaping parameters is used for both settings. We emphasize that the gain is not due to the different decoding metrics (BMD vs. SMD) as suggested by the asymptotic Shannon limits in Table I.

Fig. 4 shows simulation results for  $n_{c,\text{bin}} = 768$  bits and  $R_t = 2.0$  bpcu. As before, we see a clear improvement of 0.35 dB over the binary LDPC code.

Finally, Fig. 5 depicts the performance for  $n_{c,\text{bin}} = 1008$  bits and  $R_t = 2.75$  bpcu. Here, we use a 16-ASK constellation and code rate  $5/6$ . The observations from Figs. 3 and 4 also carry on to higher SEs.

## V. CONCLUSION

In this paper, we showed how to combine non-binary codes over  $\mathbb{F}_{2^p}$  with PAS. Numerical simulation results with ultra-sparse high order NB-LDPC codes show a significant improvement of up to 0.63 dB over state-of-the-art binary LDPC codes combined with PAS for the shortest considered blocklength of 576 bits at a FER of  $10^{-3}$ . For future research, we plan to tackle the issue of code design using a protograph based approach to take the different variable node input prob-

TABLE I  
SUMMARY OF THE SHAPED MODES USED IN THE NUMERICAL SIMULATION RESULTS.

Mode	M	$R_c$	$k/n$	$R_{dm}$	$\gamma$	SNR <sub>CAP</sub> [dB]	SNR <sub>SMD</sub> [dB]	SNR <sub>BMD</sub> [dB]
8-ASK, $R_t = 1.5$ bpcu	8	3/4	240/192	1.25	1/4	8.451	8.462	8.484
8-ASK, $R_t = 2.0$ bpcu	8	3/4	448/256	1.75	1/4	11.761	11.898	11.920
16-ASK, $R_t = 2.75$ bpcu	16	5/6	609/252	2.4167	1/3	16.460	16.497	16.512

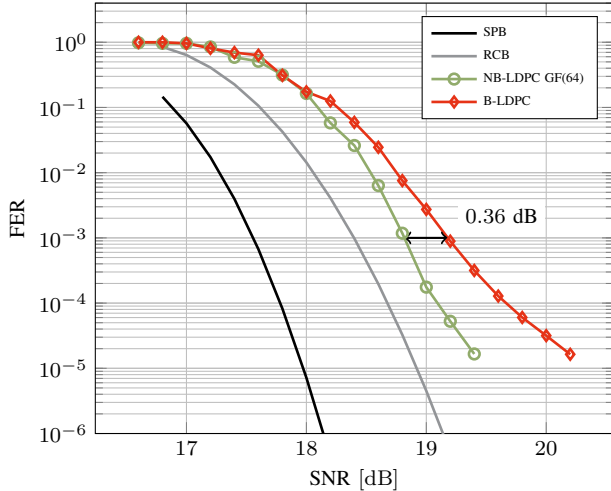


Fig. 5. Simulation results of suggested NB-LDPC coding scheme for 16-ASK,  $R_t = 2.75$  bpcu and binary blocklength of  $n_{c,bin} = 1008$  bits.

ability mass functions (PMFs) into account (see (9), (10)). For instance, we combine the approaches of [30]–[32]. Additional work should also focus on code designs for smaller field sizes to decrease the decoding complexity, see e.g., [12].

## REFERENCES

- [1] G. Forney, R. Gallager, G. Lang, F. Longstaff, and S. Qureshi, “Efficient Modulation for Band-Limited Channels,” *IEEE J. Sel. Areas Commun.*, vol. 2, no. 5, pp. 632–647, Sep. 1984.
- [2] G. Böcherer, F. Steiner, and P. Schulte, “Bandwidth Efficient and Rate-Matched Low-Density Parity-Check Coded Modulation,” *IEEE Trans. Commun.*, vol. 63, no. 12, pp. 4651–4665, Dec. 2015.
- [3] P. Schulte and G. Böcherer, “Constant Composition Distribution Matching,” *IEEE Trans. Inf. Theory*, vol. 62, no. 1, pp. 430–434, Jan. 2016.
- [4] F. Buchali, F. Steiner, G. Böcherer, L. Schmalen, P. Schulte, and W. Idler, “Rate Adaptation and Reach Increase by Probabilistically Shaped 64-QAM: An Experimental Demonstration,” *J. Lightw. Technol.*, vol. 34, no. 7, pp. 1599–1609, Apr. 2016.
- [5] W. Idler, F. Buchali, L. Schmalen, E. Lach, R. P. Braun, G. Böcherer, P. Schulte, and F. Steiner, “Field Trial of a 1 Tbit/s Super-Channel Network Using Probabilistically Shaped Constellations,” *J. Lightw. Technol.*, vol. 35, no. 8, pp. 1399–1406, 2017.
- [6] J. Cho, X. Chen, S. Chandrasekhar, G. Raybon, R. Dar, L. Schmalen, E. Burrows, A. Adamiecki, S. Corteselli, Y. Pan, D. Correa, B. McKay, S. Zsigmond, P. Winzer, and S. Grubb, “Trans-Atlantic Field Trial Using Probabilistically Shaped 64-QAM at High Spectral Efficiencies and Single-Carrier Real-Time 250-Gb/s 16-QAM,” in *Proc. Optical Fiber Commun. Conf. (OFC)*, Mar. 2017, paper Th5B.3.
- [7] “Signal Shaping for QAM Constellations,” Huawei, Athens, Greece, Tech. Rep., Feb. 2018, 3GPP TSG-RAN no. 88.
- [8] T. Prinz, P. Yuan, G. Böcherer, F. Steiner, O. Iscan, R. Böhnke, and W. Xu, “Polar Coded Probabilistic Amplitude Shaping for Short Packets,” in *IEEE Int. Workshop Signal Process. Advances Wireless Commun. (SPAWC)*, 2017.
- [9] G. Durisi, T. Koch, and P. Popovski, “Toward Massive, Ultrareliable, and Low-Latency Wireless Communication With Short Packets,” *Proc. IEEE*, vol. 104, no. 9, pp. 1711–1726, Sep. 2016.
- [10] B. Y. Chang, D. Divsalar, and L. Dolecek, “Non-binary protograph-based LDPC codes for short block-lengths,” in *Proc. IEEE Inf. Theory Workshop (ITW)*, Lausanne, Sep. 2012, pp. 282–286.
- [11] G. Liva, E. Paolini, B. Matuz, S. Scalise, and M. Chiani, “Short Turbo Codes over High Order Fields,” *IEEE Trans. Commun.*, vol. 61, no. 6, pp. 2201–2211, Jun. 2013.
- [12] L. Dolecek, D. Divsalar, Y. Sun, and B. Amiri, “Non-Binary Protograph-Based LDPC Codes: Enumerators, Analysis, and Designs,” *IEEE Trans. Inf. Theory*, vol. 60, no. 7, pp. 3913–3941, Jul. 2014.
- [13] J. J. Boutros, F. Jardel, and C. Méasson, “Probabilistic Shaping and Non-Binary Codes,” *arXiv:1701.07976 [cs, math]*, Jan. 2017.
- [14] M. C. Davey and D. MacKay, “Low-density parity check codes over GF(q),” *IEEE Commun. Lett.*, vol. 2, no. 6, pp. 165–167, Jun. 1998.
- [15] X. Y. Hu and E. Eleftheriou, “Cycle Tanner-graph codes over GF(2<sup>m</sup>),” in *Proc. IEEE Int. Symp. Inf. Theory (ISIT)*, Jun. 2003, pp. 87–.
- [16] C. Poulliat, M. Fossorier, and D. Declercq, “Design of regular (2, S<sub>d</sub>, c<sub>S</sub>)-LDPC codes over GF(q) using their binary images,” *IEEE Trans. Commun.*, vol. 56, no. 10, pp. 1626–1635, Oct. 2008.
- [17] W. Peterson and E. Weldon, *Error-Correcting Codes*. MIT Press, 1972.
- [18] L. Barnault and D. Declercq, “Fast decoding algorithm for LDPC over GF(2<sup>q</sup>),” in *Proc. IEEE Inf. Theory Workshop (ITW)*, Paris, Mar. 2003, pp. 70–73.
- [19] F. Steiner and G. Böcherer, “Comparison of Geometric and Probabilistic Shaping with Application to ATSC 3.0,” in *Int. ITG Conf. Source Channel Coding*, Hamburg, Germany, Feb. 2017.
- [20] F. Kschischang and S. Pasupathy, “Optimal nonuniform signaling for Gaussian channels,” *IEEE Trans. Inf. Theory*, vol. 39, no. 3, pp. 913–929, May 1993.
- [21] F. Gray, “Pulse code communication,” U. S. Patent 2632058, 1953.
- [22] G. Böcherer, “Achievable rates for shaped bit-metric decoding,” *arXiv preprint 1410.8075v6*, 2016.
- [23] R. Tanner, “A recursive approach to low complexity codes,” *IEEE Trans. Inf. Theory*, vol. 27, no. 5, pp. 533–547, Sep. 1981.
- [24] A. Venkiah, D. Declercq, and C. Poulliat, “Design of cages with a randomized progressive edge-growth algorithm,” *IEEE Commun. Lett.*, vol. 12, no. 4, pp. 301–303, Apr. 2008.
- [25] C. E. Shannon, “Probability of error for optimal codes in a Gaussian channel,” *Bell Syst. Tech. J.*, vol. 38, no. 3, pp. 611–656, May 1959.
- [26] R. G. Gallager, *Information Theory and Reliable Communication*. John Wiley & Sons, Inc., 1968.
- [27] “LDPC for eMBB and uRLLC,” Qualcomm Inc., Lisbon, Portugal, Tech. Rep., Oct. 2016.
- [28] J. Thorpe, “Low-density parity-check (LDPC) codes constructed from protographs,” *IPN progress report*, vol. 42, no. 154, pp. 42–154, 2003.
- [29] X.-Y. Hu, E. Eleftheriou, and D. M. Arnold, “Regular and irregular progressive edge-growth Tanner graphs,” *IEEE Trans. Inf. Theory*, vol. 51, no. 1, pp. 386–398, Jan. 2005.
- [30] A. Bannatan and D. Burshtein, “Design and analysis of nonbinary LDPC codes for arbitrary discrete-memoryless channels,” *IEEE Trans. Inf. Theory*, vol. 52, no. 2, pp. 549–583, Feb. 2006.
- [31] B.-Y. Chang, L. Dolecek, and D. Divsalar, “EXIT chart analysis and design of non-binary protograph-based LDPC codes,” in *Proc. IEEE Mil. Commun. Conf. (MILCOM)*, Nov. 2011, pp. 566–571.
- [32] F. Steiner, G. Böcherer, and G. Liva, “Protograph-Based LDPC Code Design for Shaped Bit-Metric Decoding,” *IEEE J. Sel. Areas Commun.*, vol. 34, no. 2, pp. 397–407, Feb. 2016.